Kinetic arrest of direct and reverse martensitic transformation and exchange bias effect in $Mn_{49.5}Ni_{40.4}In_{10.1}$ melt spun ribbons

J. L. Sánchez Llamazares, B. Hernando, J. J. Suñol, C. García, and C. A. Ross

Citation: Journal of Applied Physics **107**, 09A956 (2010);
View online: https://doi.org/10.1063/1.3357407
View Table of Contents: http://aip.scitation.org/toc/jap/107/9
Published by the American Institute of Physics

Kinetic arrest of direct and reverse martensitic transformation and exchange bias effect in $Mn_{49.5}Ni_{40.4}In_{10.1}$ melt spun ribbons

J. L. Sánchez Llamazares,[1,a)] B. Hernando,[2] J. J. Suñol,[3] C. García,[4] and C. A. Ross[4]
[1]*División de Materiales Avanzados, IPICYT, 78216, San Luis Potosi S.L.P., Mexico*
[2]*Departamento de Física, Universidad de Oviedo, Calvo Sotelo s/n, 33007 Oviedo, Spain*
[3]*Universidad de Girona, Campus de Montilivi, edifici PII. Lluís Santaló s/n. 17003 Girona, Spain*
[4]*Department of Materials Science and Engineering, MIT, Massachusetts 02139, USA*

(Presented 19 January 2010; received 31 October 2009; accepted 17 December 2009; published online 14 May 2010)

Phase coexistence phenomena related to direct and reverse martensitic transformation have been studied in melt spun ribbons of the magnetic shape memory alloy $Mn_{49.5}Ni_{40.4}In_{10.1}$. For magnetic fields above 10 kOe martensitic transformation undergoes a progressive kinetic arrest. The metastable character of the field-cooled frozen fraction of austenite into martensite was verified. An atypical incomplete reverse martensitic transformation of thermal origin was also observed. The zero-field cooled thermomagnetization curve measured at 50 kOe shows a decrease below 30 K that was accompanied by the occurrence of exchange bias effect suggesting the strengthening of antiferromagnetic interactions in martensite in such temperature range. © *2010 American Institute of Physics*. [doi:10.1063/1.3357407]

In the last few years much attention has been directed to the study of reverse martensitic transformation (MT) in the ferromagnetic (FM) shape memory alloy (FSMA) system $Ni_{50}Mn_{50-x}In_x$. Associated to the magnetostructural transition and the magnetic properties of austenite (AST) and martensite (MST) functional properties of considerable technological interest such as magnetic superelasticity, large inverse and conventional magnetocaloric effect, large magnetoresistance, and exchange bias effect, have been reported.[1–3]

Melt spun ribbons of the Heusler alloy $Mn_{49.5}Ni_{40.4}In_{10.1}$ crystallize into a single phase AST with the $L2_1$-type structure that with the lowering of temperature (T) undergoes a MT into a 14-layered modulated (14M) monoclinic MST phase .[4] This novel Mn-rich Heusler alloy shows martensitic and austenitic start and finish transition temperatures (M_S, M_f and A_S, A_f, respectively) and Curie point of AST T_C^A of M_S=213 K, M_f=173 K, A_S=222 K, A_f=243 K, and T_C^A =311 K, being an addition to the existing FSMA in the Ni–Mn–In system. The present study was designed to investigate the effect of magnetic field H on the MT as well as the split observed between field-heated (FH) and field-cooled (FC) magnetization curve in the austenitic existence region.[4] It is concluded that both behaviors are related to the incompleteness of the structural phase transition.

Details of the sample preparation and basic magnetostructural characterization of AST and MST phases have been described earlier.[4] Magnetization (M) and resistivity (ρ) measurements were made by means of a physical properties measurement system (Quantum Design, PPMS-9T). H was applied along the rolling direction to minimize demagnetizing field effect. XRD analyses were performed using Cu Kα radiation with a low temperature diffractometer.

Figure 1 shows the $M(T)$ plot of the sample in zero-field cooling (ZFC), FC, and FH modes for H=10, 50, and 80 kOe (2 K/min). Upon heating at H=10 kOe [Fig. 1(a)], $M^{ZFC}(T)$ curves first registered an initial rise in the low T range followed by a slight decreasing tendency until the reverse MT occurs. The latter one is marked by the sudden and substantial rise in M due to the strengthening of FM correlations in the AST phase that leads to its higher saturation magnetization. It must be noticed that above A_f there is a non-negligible difference between $M^{ZFC}(T)$ and $M^{FC}(T)$ curves that suggests the incompleteness of the reverse MT. The effect is also present at 50 and 80 kOe even when the phase transition is shifted toward lower temperatures. The nature of

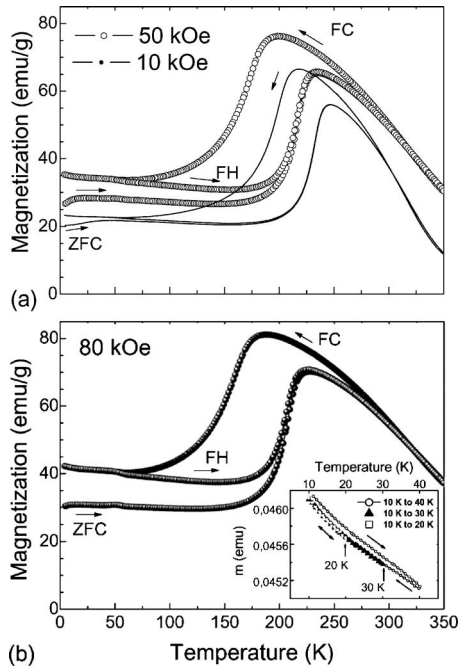

FIG. 1. $M(T)$ plots under H=10 and 50 kOe (a) and 80 kOe (b). The inset in (b) shows the effect of thermal cycling between 10 and 40 K (open circles), 10–30 K (full triangles), and 10–20 K (open squares) on the FC m(T) under H=80 kOe.

a)Author to whom correspondence should be addressed. Electronic mail: sanchez@nanomagnetics.org.

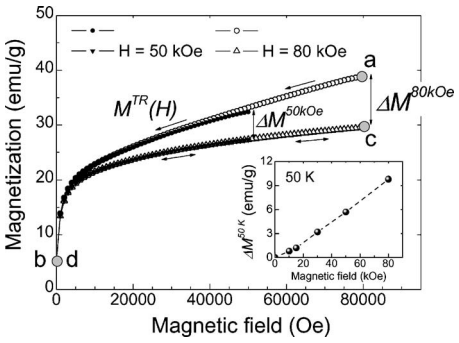

FIG. 2. $M^{TR}(H)$ and subsequent field-up and field-down isotherms at 50 K obtained after FC the sample from 350 K in presence of $H_{max}=50$ and 80 kOe. The vertical double arrow indicates the irreversible magnetization change ΔM for both H_{max} values. Inset: ΔM at 50 K vs H.

this phenomenon will be described below. Notice that AST to MST transition occurs in a broad temperature range, shows a large thermal hysteresis and the $M^{FC}(T)$ curve at 10 kOe tends to seek $M^{ZFC}(T)$ below 70 K. Below 70 K $M^{FH}(T)$ retraces $M^{FC}(T)$ and above such T is overlapped with $M^{ZFC}(T)$ until 350 K. In contrast, when $H=50$ and 80 kOe [Fig. 1(a) and 1(b)] there is a distinct difference between $M^{ZFC}(T)$ and both the $M^{FC}(T)$ and $M^{FH}(T)$ pathways that exhibit higher M values. In fact, $M^{FH}(T)$ and $M^{ZFC}(T)$ run nearly reciprocally parallel from 4 K to A_S. These results suggest that the first-order MT is arrested for H beyond a certain critical value. The kinetic arrest of MT gives rise to a magnetically inhomogeneous system in which magnetic MST and AST phases coexist. The kinetic arrest of the MT suggests that, by effect of H, nonequilibrium AST regions remain frozen into an equilibrium MST matrix. Thus, the resulting FC state should be metastable in nature and therefore if H is removed or thermal fluctuations are introduced the system should tend to the ZFC state. To prove this two further measurements were made. First, the sample was heated to 350 K and then FC under $H=80$ kOe until $T=10$ K. Keeping H a successive cycling of the temperatures among 10–40 K, 10–30 K, and 10–20 K was performed to introduce thermal energy fluctuations. The inset of Fig. 1(b) shows that the first energy fluctuation up to 40 K caused a small but detectable irreversible decay in the magnetic moment m at 80 kOe suggesting the metastable character of the FC state. However, subsequent thermal cycles from 10 to 30 K (or 20 K) no further decreased m. A further experiment consisted in cooling the sample from 350 K under $H=50$ and 80 kOe, respectively, until 50 K (i.e., below 70 K), in order to measure the demagnetization $M^{TR}(H)$ curve (usually referred in literature to as thermoremanent demagnetization curve)[5] followed by the subsequent field-up and field-down isotherms. Figure 2 shows the irreversible character of $M^{TR}(H)$ with respect to the reversible one of the successive $M(H)$ curves [we stated in the figure that for $H_{max}=80$ kOe$M(H)$ followed the paths a-b, b-c, and c-d]. The maximum M difference, $\Delta M^{50\ kOe}$ and $\Delta M^{80\ kOe}$, is indicated in the figure. It is in excellent agreement with the one computed from the respective $M(T)$ curve taken at 50 K. The inset of Fig. 2 shows that $\Delta M(H)$ increases almost linearly with H increasing. The latter one suggests that the frozen faction of AST in the FC

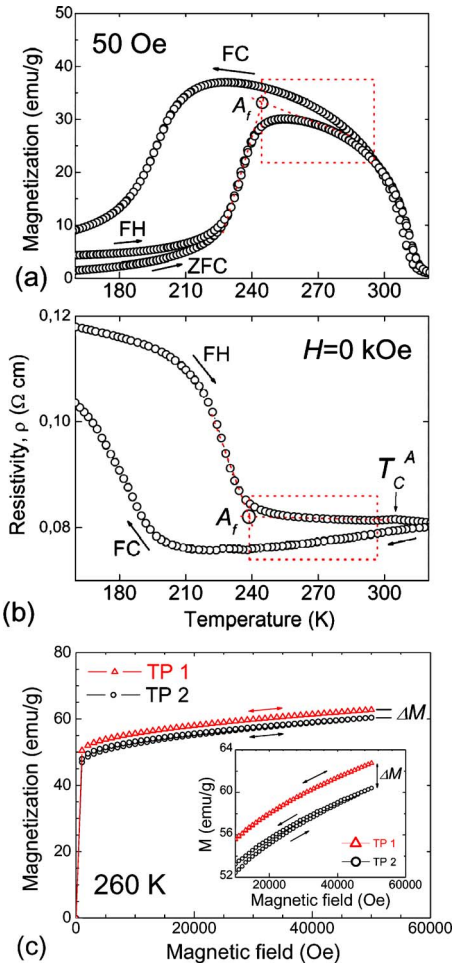

FIG. 3. (Color online) $M(T)$ curve measured at 50 Oe (a) and $\rho(T)$ curve at zero-field (b) in the range of $170\leq T\leq 310$ K. (c) Field-up and field-down $M(H)$ curves at 260 K after reaching this temperature following TP1 and TP2. Inset: high-field region of the curves.

state is proportional to the H value. These results show that indeed the FC low temperature state exiting in the martensitic existence region is metastable. By removing H the metastable fraction of AST coexisting with the converted fraction of equilibrium MST progressively transforms into MST and therefore the FC state tends to the ZFC one. Also notice that the curves measured up to $H_{max}=50$ kOe practically overlap with those measured up to 80 kOe.

The kinetic arrest of the MT transformation, has been also observed in other magnetic materials showing thermal and field-induced magnetostructural transitions such as Ru-doped $CeFe_2$ (Ref. 6) and manganite compounds.[7] It has been also reported for two other Heusler FSMA alloys derived from the ternary Ni–Mn–In system, namely, $Ni_{50}Mn_{14}In_{16}$ (Ref. 5) and $Ni_{45}Co_5Mn_{36.7}In_{13.3}$.[8] In both cases samples were bulk alloys.

Another intriguing feature of this alloy ribbons is the distinctive and noteworthy difference between $M^{ZFC}(T)$ and $M^{FC}(T)$ curves above A_S in the austenitic existence region [moreover, $M^{FH}(T)$ replicates $M^{ZFC}(T)$ curve]. This behavior is also observed in the $M(T)$ curves plotted in Fig. 1 for different H values. Figures 3(a) and 3(b) show the ZFC, FC, and FH $M(T)$ curve in $H=50$ Oe and FH and FC $\rho(T)$ curve

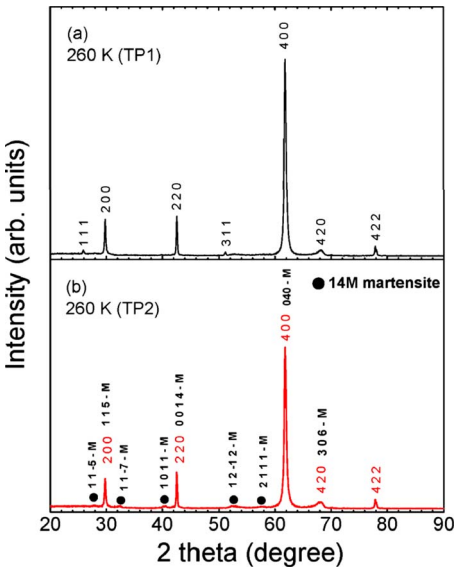

FIG. 4. (Color online) X-ray powder diffraction pattern obtained at 260 K after reaching this temperature following TP1 (a) and TP2 (b).

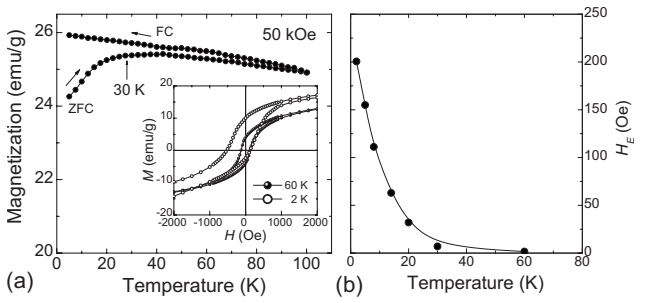

FIG. 5. (a) ZFC and FC $M(T)$ curves at 50 kOe in the temperature range of 4 K $\leq T \leq$ 100 K. Inset: low-field region of the FC hysteresis loops at 2 and 60 K. (b) Temperature dependence of the exchange bias field H_E.

in zero-field in the range $170 \leq T \leq 310$ K, respectively. The T range where the mismatch between $M^{ZFC}(T)$ $[M^{FH}(T)]$ and $M^{FC}(T)$ occurs is indicated by the dashed rectangles traced. Notice that in the T interval where the material shows a lower M a higher ρ is obtained; moreover, the FH $\rho(T)$ path is relatively flat in contrast with that of the FC $\rho(T)$ path that shows a linear and positive slope (suggesting a difference in the conductivity characteristic). To obtain further information on the thermal nature of this behavior, Fig. 3(c) shows field-up and field-down $M(H)$ curves at 260 K after reaching this temperature following two thermal protocols (TP1 and TP2); the high-field region of the curves is plotted in the inset. In TP1 the sample reached $T=260$ K by ZFC from 350 K and in TP2 is first heated to 350 K, cooled in $H=0$ to 10 K, and then to $T=260$ K. Both curves are quite similar running parallel one to each other, but that obtained after TP2 shows a lower saturation magnetization. These results points to the incompleteness of the MST-to-AST transformation. This unusual phase coexistence phenomenon has thermal nature and implies that a fraction of MST remains frozen coexisting with the majority AST. With the increase in T the volume fraction of frozen MST progressively transforms into AST explaining the behavior of both $M(T)$ and $\rho(T)$ curves. Figures 4(a) and 4(b) show XRD spectra at 260 K after TP1 and TP2, respectively. The XRD spectrum of Fig. 4(a) shows that the sample is a single phase with the $L2_1$ structure. However, after TP2 the XRD pattern [Fig. 4(b)] shows the appearance of several weak reflections that belong to the low temperature 14M MST confirming its phase coexistence as minor phase with the $L2_1$ AST.

Finally, we studied the origin of the broad peak around 30 K observed in the high-field $M^{ZFC}(T)$ curve. So, the sample was first prepared in ZFC state and the ZFC and FC $M(T)$ curves from 4 to 100 K were measured at $H=50$ kOe (i.e., the thermal cycle was performed within the MST existence region). From Fig. 5(a) we observe that $M^{ZFC}(T)$ undergoes a rise up to around 30 K followed by a smooth decrease of M. In contrast, $M^{FC}(T)$ tends to behave linearly with a similar negative slope and does not merge with the $M^{ZFC}(T)$. Below 30–40 K the difference $M^{FC}(T)$-$M^{ZFC}(T)$ increases with the decreasing of T. This behavior may arise from the strengthening of anti-FM (AFM) interactions within MST. The coexistence of AFM and FM correlations within MST regions, also referred as the occurrence of magnetic inhomogeneous states, has been stated as the origin of the exchange bias (EB) effect reported at low temperatures in bulk $Ni_{50}Mn_{50-x}In_x$ alloys.[3] Then we measured FC hysteresis loops below 60 K. In order to avoid any phase coexistence associated to the kinetic arrest phenomenon that could affect a correct determination of the loops, the sample was heated to 350 K, ZFC to 100 K where $H=20$ kOe is applied, and then FC to each measuring temperature. The inset of Fig. 5(a) shows the low-field region of the FC hysteresis loop at 2 and 60 K. The loop at 2 K shifts along the negative H-axis direction confirming the occurrence of EB effect. Figure 5(b) displays the temperature dependence of H_E. Notice both, that the H_E field shows a rapid T decreasing and the T interval where the phenomenon occurs is almost coincident with that in which a decreasing of $M^{ZFC}(T)$ is observed.

In conclusion, two different phase coexistence phenomena occur in ribbons of the FSMA $Mn_{49.5}Ni_{40.4}In_{10.1}$. One of them is the kinetic arrest of MT and takes place when the alloy is FC under $H>10$ kOe. The amount of AST phase frozen into the MST matrix rises with the increasing of H. The metastable character of the FC state was demonstrated. The other one has a thermal origin and also represents a kinetic arrest of the reverse MT. The coexisting fraction of MST decreased with the increases of T. The common feature of both events is phase coexistence and metastability that is a primary characteristic of all disorder-influenced, first-order phase transitions. Lastly, EB effect was observed below 30 K suggesting the coupling between AFM and FM interfaces in the martensitic state.

We acknowledge MICINN (Project No. MAT2009-13108-C02-01 and 02) and Fulbright program (C. Garcia).

[1]A. Planes *et al.*, J. Phys.: Condens. Matter **21**, 233201 (2009).
[2]S. Y. Yu *et al.*, Appl. Phys. Lett. **89**, 162503 (2006).
[3]B. M. Wang *et al.*, J. Appl. Phys. **104**, 043916 (2008).
[4]J. L. Sánchez Llamazares *et al.*, Appl. Phys. Lett. **92**, 012513 (2008).
[5]V. K. Sharma *et al.*, Phys. Rev. B **76**, 140401(R) (2007).
[6]M. K. Chattopadhyay *et al.*, Phys. Rev. B **72**, 180401(R) (2005).
[7]K. Kumar *et al.*, Phys. Rev. B **73**, 184435 (2006).
[8]W. Ito *et al.*, Appl. Phys. Lett. **92**, 021908 (2008).